Quantitative assessment of the functional plasticity of memory CD8$^+$ T cells

Adriana Baz[*], Penny Groves, Kathy Buttigieg[**], Simon H. Apte, Norbert Kienzle[***] and Anne Kelso[****]

Cooperative Research Centre for Vaccine Technology, QIMR Berghofer Medical Research Institute, QLD, Australia

Keywords: Plasticity, memory, CD8$^+$ T cells, IL-4, IFN-γ

Correspondence: Prof Anne Kelso, Department of Microbiology and Immunology, The University of Melbourne, at the Peter Doherty Institute for Infection and Immunity, 792 Elizabeth St, Melbourne, VIC 3000, Australia. Tel: +61-3-8344 3437; Fax: +61-3-9347 1540; e-mail: akelso@unimelb.edu.au

Abbreviations: DMEM: Dulbecco's modified Eagle's medium; FCS: fetal calf serum; FITC: fluorescein isothiocyanate; MEM: Dulbecco's minimal essential medium; PE, phycoerythrin.

[*] Present address: CSL Limited, 45 Poplar Rd, Parkville, VIC 3052, Australia

[**] Present address: Menzies Institute for Medical Research, University of Tasmania

Private Bag 23, Hobart, TAS 7000, Australia

[***] Present address: Ingham Institute for Applied Medical Research, Liverpool, NSW 2170, Australia

[****] Present address: Department of Microbiology and Immunology, The University of Melbourne, at the Peter Doherty Institute for Infection and Immunity, 792 Elizabeth St, Melbourne, VIC 3000, Australia

Abstract

While the functional plasticity of memory $CD4^+$ T cells has been studied extensively, less is known about this property in memory $CD8^+$ T cells. Here we report the direct measurement of plasticity by paired daughter analysis of effector and memory OT-I $CD8^+$ T cells primed in vivo with ovalbumin. Naïve, effector and memory OT-I cells were isolated and activated in single-cell culture then, after the first division, their daughter cells were transferred to new cultures with and without IL-4; expression of IFN-γ and IL-4 mRNAs was measured 5 days later in the resultant subclones. Approximately 40% of clonogenic memory $CD8^+$ T cells were bipotential in this assay, giving rise to an $IL\text{-}4^-$ subclone in the absence of IL-4 and an $IL\text{-}4^+$ subclone in the presence of IL-4. The frequency of bipotential cells was lower among memory cells than naïve cells but markedly higher than among 8-day effectors. Separation based on high or low expression of CD62L, CD122, CD127 or Ly6C did not identify a phenotypic marker of the bipotential cells. Functional plasticity in memory $CD8^+$ T-cell populations can therefore reflect modulation at the level of a single memory cell and its progeny.

Baz et al. Quantitative assessment of the functional plasticity of memory $CD8^+$ T cells

Graphical abstract

Whereas naïve $CD8^+$ T cells lose the ability to change cytokine profile when they differentiate into effector cells, a substantial fraction of memory cells primed in the same response display functional plasticity. Tailoring of immune function can therefore continue in the secondary response at the level of the individual memory cell.

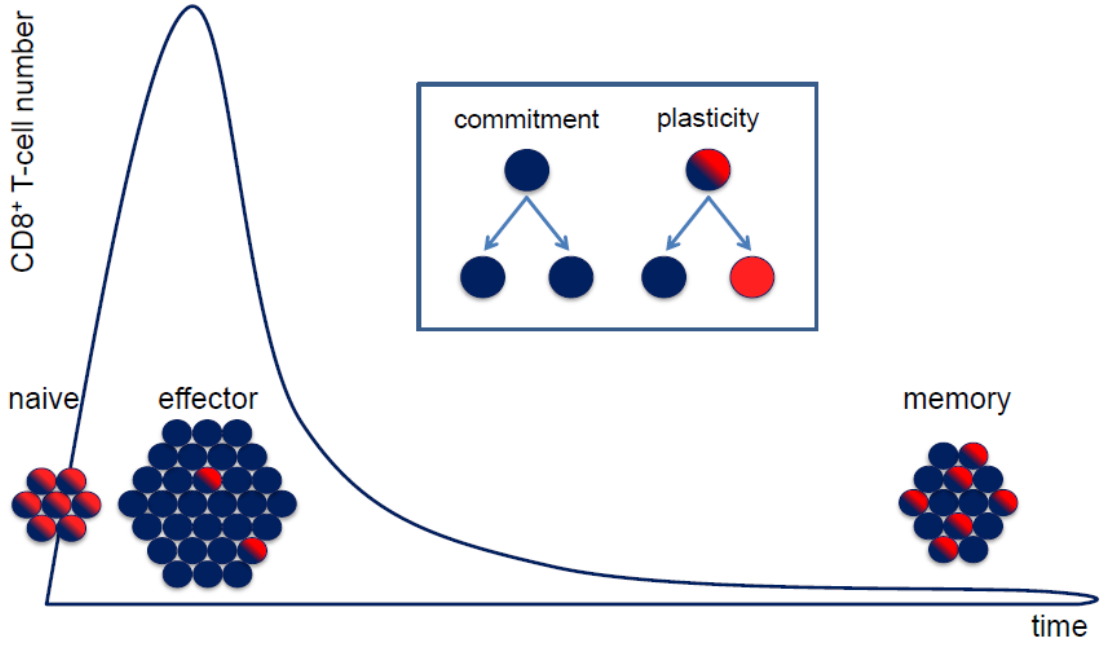

Introduction

There is currently much interest in determining whether memory T cells are programmed to express functions activated during priming, or whether they can retain functional plasticity in response to new conditions when challenged [1]. Primary $CD4^+$ T-cell populations have been shown to lose functional plasticity with extended culture in Th1 or Th2 polarizing conditions in vitro [2, 3]. This loss of plasticity is associated with positive and negative regulatory loops that maintain the polarized gene expression profile as well as heritable epigenetic modifications to transcription factor and effector genes [4]. In memory $CD4^+$ T-cell responses, on the other hand, there is evidence both for maintenance of the gene expression profile of the primary effector population and for functional plasticity, depending on re-activation conditions [5-9].

Although activated $CD8^+$ T cells typically display a type 1 cytokine profile and cytolytic activity, primary activation in the presence of IL-4 leads to development of poorly cytolytic, type 2

cytokine-producing cells at high efficiency [10, 11]. To determine whether naïve $CD8^+$ T cells were plastic, we used paired daughter analysis in which individual $CD8^+$ T cells were activated and their daughters were then separated and cloned in the presence or absence of IL-4. The data showed that most naïve peripheral $CD8^+$ T cells gave rise to subclones with different cytokine profiles depending on their exposure to IL-4 during cloning and were therefore multipotential [12]. Others have demonstrated plasticity of $CD8^+$ T-cell surface phenotype using a similar approach [13]. We further showed that effector $CD8^+$ T cells from lungs of influenza virus-infected mice also displayed functional plasticity, although at lower frequency than naïve $CD8^+$ T cells [14]. Others have reported conversion of in vitro-polarized $CD8^+$ T cells of several phenotypes into cells producing alternate cytokines following adoptive transfer in vivo [15, 16] and we have demonstrated plasticity of CpG methylation and expression of *CD8a* in effector $CD8^+$ T cells following IL-4 polarization in vitro [17]. However, while there is evidence for maintenance of cytokine profiles [18], quantitative studies of functional plasticity in memory $CD8^+$ T cells have not yet been reported.

We have now used paired daughter analysis to quantify the functional plasticity of memory $CD8^+$ T cells, using IL-4-induced IL-4 expression as the indicator. This approach has the advantage over population studies that it distinguishes cellular plasticity from preferential survival, activation or proliferation of cells already primed to express the alternate properties. We show that, under the conditions used here, the plasticity of in vivo-primed memory populations was closer to that of naïve $CD8^+$ T cells and markedly higher than that of primary effector populations activated in the same response in vivo. This suggests that many memory $CD8^+$ T cells can modulate their function in response to new signals received during challenge.

Results

Effector and memory CD8$^+$ T cells are generated in an adoptive transfer model

To enable direct comparison of in vivo-activated effector and memory CD8$^+$ T cells of the same specificity, $OVA_{257-264}$ peptide-specific TCR transgenic OT-I cells (CD45.2) were adoptively transferred into congenic CD45.1 recipient mice; the mice were then immunized one day later with irradiated OVA-coated CD45.1 splenocytes. Activated OT-I cells defined by the phenotype CD45.2$^+$CD8$^+$CD44^{high}CD62L^{low} were detected in draining LN by day 4 after priming, reached maximum number and percentage (of all OT-I cells) on day 4 – 5 and declined to baseline by day 17 (Fig. 1A). Changes in total OT-I cell numbers followed similar kinetics (data not shown). At day 5, the activated OT-I population contained effector cells able to degranulate in response to antigen (as indicated by surface CD107 expression) and cytolytic T-lymphocyte precursors able to lyse OVA-expressing target cells in an antigen-specific manner following expansion in vitro (Fig. 1B, C).

OT-I cells with an activated/memory phenotype (CD45.2$^+$CD8$^+$CD44^{high}) were detected in spleens of recipient mice for at least one year after priming (data not shown). At day 60 these cells displayed several properties of memory T cells. First, compared to naïve cells, most expressed elevated levels of the memory cell markers CD44, CD122 and Ly6C, and most were CD127^{high}CD62L^{high} (Fig. 2A). Second, they expressed memory T-cell functions when stimulated with anti-CD3 mAb for 4 h in vitro, including up-regulation of IL-2 mRNA (data not shown) and degranulation (Fig. 2B). Third, recipient mice rejected the OVA-expressing EG.7 thymoma when challenged three months after adoptive transfer of OT-I cells and OVA priming (Fig. 2C).

In the following experiments, OT-I cells isolated shortly after the peak of the primary response at day 8 and at least 60 days after in vivo priming with OVA-coated splenocytes were used as a source of effector and memory CD8$^+$ T cells respectively.

Naïve, effector and memory CD8$^+$ T-cell populations differ in their responsiveness to IL-4

To measure the functional plasticity of CD8$^+$ T cells, we took advantage of the observation that naïve CD8$^+$ T cells activated in neutral or type 1-polarizing conditions generate progeny that rarely express IL-4 whereas most of those exposed to IL-4 during activation in vitro generate IL-4-producing progeny [11, 12]. Effector and memory OT-I populations activated in the adoptive transfer model described above did not contain detectable IL-4 mRNA ex vivo (data not shown).

Purified naïve (defined as CD44^{lo}CD62L^{hi}) and in vivo-primed effector (CD44^{hi}CD62L^{lo}) and memory (CD44^{hi}CD62L^{hi}) OT-I cells from this model were activated in single-cell cultures with immobilized mAb to CD3, CD8 and CD11a (hereafter abbreviated as anti-CD3/8/11a Ab) and IL-2 in the presence or absence of IL-4. This clonal system supports development of CD8$^+$ T-cell clones from naïve cells at high efficiency [11, 12], allows responsive cells to be quantified and reduces cross-regulation by endogenous cytokines which counteract IL-4 in bulk cultures. When clones had developed 5 days later, their size was estimated and clones of a range of sizes were analyzed for expression of CD3ε, IFN-γ and IL-4 mRNA by two-round nested RT-PCR (Table 1). Cloning efficiency and average clone size were highest for naïve cells, intermediate for memory cells and lowest for effector cells. CD3ε and IFN-γ mRNAs were detected in all tested clones. Consistent with our earlier analyses [12, 14], most clones generated from naïve cells in the presence of IL-4 expressed IL-4 mRNA (mean of 96% compared with 8% in the absence of IL-4), whereas only 19% of clones derived from effector cells expressed IL-4 under these conditions. Surprisingly, 84% of memory cell clones expressed IL-4 in the presence of IL-4, compared with 7% in its absence. These data suggested that the functional plasticity of in vivo-activated OT-I memory cells was higher than that of primary effectors from the same response and approached the levels observed here in naïve OT-I cells and in WT CD8$^+$ T cells [12, 14].

Paired daughter analysis demonstrates the existence of bipotential CD8$^+$ memory T cells

It was possible that the high frequency of IL-4 expression among memory cell-derived clones described above reflected selective expansion of pre-existing IL-4-expressing memory cells in the presence of IL-4, rather than reprogramming of IL-4-negative cells. We therefore used paired daughter analysis [12, 14] to measure directly the plasticity of individual memory cells.

Single purified naïve, effector and memory cells were cultured with anti-CD3/8/11a Ab and IL-2 (Fig. 3A). After the first division, individual daughter cells were transferred by micromanipulation to new wells and cultured with or without IL-4. Five days later the number of cells per subclone was estimated and pairs of subclones generated from the same parent cell were assayed for expression of CD3ε, IFN-γ and IL-4 mRNA (Table 2). The initial cloning efficiency of memory cells was intermediate between that of naïve cells and of effector cells (p <0.0001 for each two-way comparison), as observed above (Table 1). After daughter cell transfer, both cloning efficiency and mean subclone size were generally lowest for memory cells. All tested subclones contained detectable CD3ε mRNA and most contained IFN-γ mRNA. Very few subclones of any cell type expressed IL-4 mRNA in the absence of IL-4 exposure but, for subclones grown in the presence of IL-4, the frequency of IL-4 expressers was highest among those derived from naïve cells and lowest among those derived from effector cells (Table 2). Analysis of cytokine co-expression (Fig. 3B) showed that all IL-4$^+$ subclones also expressed IFN-γ whether or not they were grown in the presence of IL-4.

When the IL-4 expression data for daughter pairs were aligned (Fig. 3C), only three of the four possible outcomes were observed: (1) both daughters gave rise to IL-4-negative subclones (-/-), (2) both gave rise to IL-4-positive subclones (+/+) or (3) the daughter in IL-2 gave rise to an IL-4-negative subclone and its sister in IL-2+IL-4 gave rise to an IL-4-positive subclone. The fourth possibility (+/-) was not observed. The data suggest that parent cells which gave rise to -/- subclones

were committed to an IL-4-nonproducer phenotype, while parents that gave rise to +/+ subclones were already committed to IL-4 production, eg due to IL-4 exposure during priming or, in the case of naïve cells, because they were responsive to an IL-4-independent trigger of IL-4 production. Cells that gave rise to an IL-4-negative subclone in the absence of IL-4 and an IL-4-positive subclone in the presence of IL-4 were considered bipotential (functionally plastic); their frequency was highest among naïve cells, intermediate among memory cells and lowest among effector cells (Table 2) (p <0.0001 for each two-way comparison).

The bipotential cell frequencies obtained by paired daughter analysis followed the same hierarchy suggested by the clonal studies in Table 1, although numerically lower for all three populations, particularly for memory cells. Memory cells also yielded lower cloning efficiencies and mean clone sizes in the paired daughter protocol than in clonal studies, suggesting they may be less able to withstand micromanipulation and re-culture than the daughters of naïve and effector cells.

Bipotential memory cells lack a distinctive cell surface phenotype

Memory cells in the model used here were phenotypically heterogeneous (Fig. 2A). To investigate whether IL-4-responsive (bipotential) cells could be distinguished from other cells in the memory pool, $CD45.2^{+}CD8^{+}CD44^{high}$ cells from spleens of adoptively transferred and OVA-primed mice were separated based on high or low expression of CD62L, CD122, CD127 or Ly6C, and cloned in the presence or absence of IL-4. Cloning efficiencies and clones sizes were generally comparable for cells expressing high or low levels of each marker (Table 3). For all markers tested, both high and low expressing populations gave rise to IL-4-positive clones at markedly higher frequency in the presence of IL-4 than in its absence (although we observed an unexpectedly high frequency of IL-4-positive clones in cultures of $Ly6C^{low}$ cells in IL-2 alone). The proportion of IL-4-responsive cells was not

significantly different between high and low expressing cells (p >0.05), suggesting that functionally plastic cells could not be distinguished using the markers examined here.

Memory cells display functional plasticity in vivo

To test the functional plasticity of memory populations in vivo, memory OT-I cells isolated 6 months after priming were transferred into RAG-1-deficient mice with IL-4-secreting or control non-secreting OVA-expressing EG.7 tumor cells. Control RAG-1-deficient mice received OT-I cells from naïve mice with IL-4-secreting or non-secreting EG.7 tumor cells. Effector OT-I cells were recovered from pooled draining LN and spleens 5 days later and assayed for IFN-γ and IL-4 mRNA (Fig. 4). In two independent experiments, IL-4 mRNA was detected in the progeny of both memory and naïve cells but only in populations from mice that received IL-4-expressing tumor cells, whereas IFN-γ mRNA levels were similar in the presence and absence of IL-4. The data support the conclusion that memory cells activated in this system retain functional plasticity in vivo.

Discussion

Here we show that some in vivo-primed, type 1-polarized memory $CD8^+$ T cells retain the capacity to express IL-4 when re-activated in the presence of IL-4. This functional plasticity was demonstrated both in single-cell cloning experiments in vitro and in response to a tumor challenge in vivo. Using paired daughter analysis to quantify IL-4-responsive cells, we further show that the frequency of these cells in the memory $CD8^+$ T-cell population studied here is substantially higher than in the corresponding effector population and closer to that of naïve $CD8^+$ T cells.

The use of paired daughter analysis was critical to show that the detection of IL-4-producing cells was due to de novo induction of IL-4 rather than selective expansion of pre-existing IL-4-producing memory cells. This protocol showed definitively that many single memory cells were bipotential: in about 42% of pairs, the daughter cultured without IL-4 generated a subclone that did not express IL-4 and the daughter cultured with IL-4 generated a subclone that expressed IL-4; the converse result was not obtained. This estimate of bipotential cell frequency among memory cells is significantly higher than that obtained for effector cells (6.1%) and nearer to that of naïve cells (73.5%) in parallel analyses. The bipotential cell frequency was also lower among effector $CD8^+$ T cells isolated from the lung parenchyma of influenza virus-infected mice than among naïve LN $CD8^+$ T cells in our earlier study [14].

Both the absolute and relative functional plasticity of effector and memory T cells are likely to depend on the nature and dose of the immunogen, TCR affinity, T-cell precursor frequency, division number and other variables. We have, however, obtained qualitatively similar results in another model in which endogenous, rather than adoptively transferred, T cells are primed by a replicating, rather than a non-replicating, immunogen in a different mouse strain. Intraperitoneal injection of DBA/2 mice with HLA-CW3-transfected P815 tumor cells preferentially activates endogenous TCR Vβ10-

bearing $CD8^+$ T cells specific for the HLA-$CW3_{170-179}$ epitope leading to tumor clearance over 12 – 15 days [19, 20]. Using either anti-Vβ10 mAb or H-$2K^d$/$CW3_{170-179}$ tetramers to purify the responding cells, paired daughter analysis of these type 1-polarized effector and memory $CD8^+$ T cells showed that 30 – 35% of memory cells were bipotential, compared with 0 – 12% of day-12 effector cells (K. Buttigieg, P. Groves, A. Kelso, unpublished observations).

Memory $CD8^+$ T cells are phenotypically and functionally heterogeneous. High and low expression of the LN homing receptor CD62L (and CCR7) distinguishes central and effector memory $CD8^+$ T cells, which differ in circulation, location and expression of immediate effector functions [21]. Memory cells can also be subdivided based on expression of CD122 (IL-2Rβ) and CD127 (IL-7Rα), which are required for homeostatic proliferation and survival of most memory cells, and Ly6C, which is associated with LN homing of central memory $CD8^+$ T cells [22, 23]. However, separation of memory $CD8^+$ T cells expressing high or low CD62L, CD122, CD127 or Ly6C did not enrich or deplete IL-4-responsive cells in the system used here. Work is continuing to search for phenotypic markers of plasticity among memory $CD8^+$ T cells that would assist in their molecular characterization.

Our findings have implications for understanding the development and regulation of immunological memory. Memory $CD8^+$ T cells have been postulated to arise directly from effector cells that survive the contraction phase after antigen clearance and/or from precursor memory cells that diverge from the effector pathway during the primary response, for example by asymmetric division of the earliest responding cells [24-27]. The fate of individual $CD8^+$ T cells activated during the primary response is influenced by many intrinsic and extrinsic factors that drive activation and repression of gene expression and establish heritable epigenetic modifications that coordinate and stabilise these transcriptional programs [4, 28]. As epigenetic modifications would be expected to favour re-expression of the cell's original effector functions by its progeny when challenged [29-31],

our data at first glance support the idea that functionally plastic memory cells are not derived directly from primary effector cells but instead represent a distinct lineage of less differentiated cells.

There is, however, growing evidence that some activated $CD4^+$ and $CD8^+$ T cells retain epigenetic plasticity [8, 16, 17]. For example, we reported recently that IL-4-induced down-regulation of surface CD8αβ during primary $CD8^+$ T cell activation was associated with re-methylation of the *CD8a* locus but that IFN-γ could reverse this effect in some $CD8^{low}$ cells, promoting CD8 re-expression and *CD8a* demethylation in their progeny [17]. Therefore, functional plasticity in memory $CD8^+$ T cells may reflect persistent epigenetic plasticity, even when memory cells develop directly from effectors. Bivalent histone modifications in key regulatory genes (such as *Tbx21* and *Gata3*) that poise T cells for rapid gene expression or repression in response to external signals offer one mechanism that could underlie the functional plasticity of memory T cells [8, 28, 32, 33].

In conclusion, our data directly demonstrate that functional plasticity in memory populations can reflect modulation at the level of a single memory $CD8^+$ T cell and its progeny, rather than by selective recruitment from a heterogeneous memory cell pool. The evolutionary importance of plasticity among memory $CD8^+$ T cells is unknown but, in principle, it would allow the continued tailoring of immune function during secondary responses, as shown here in the response to an IL-4-expressing tumor in vivo. Understanding of the regulation and molecular basis of this plasticity may therefore present opportunities to reprogram ineffective or pathogenic recall responses in the memory phase.

Materials and Methods

Mice

Specific pathogen-free C57BL/6 (CD45.2), B6.SJL/J-Ptprc^{a} (CD45.1) and RAG-1$^{-/-}$ mice (Animal Resources Centre, Perth, WA, Australia) and OT-I (243.2) TCR-transgenic mice [34] (provided by W.R. Heath, The Walter and Eliza Hall Institute of Medical Research, Victoria, Australia) were used at 5–10 weeks of age. All animal experiments were approved by the QIMR Animal Ethics Committee.

Purification, adoptive transfer and priming of OT-I cells

OT-I cells were prepared by passing pooled OT-1 spleens and axillary, brachial, inguinal and lumbar LN through stainless steel mesh, red blood cell lysis with 0.9% NH_4Cl and centrifugation on Ficoll-Paque (Amersham Biosciences, SA, Australia). CD8^{+} T cells were enriched by magnetic depletion using mAb to MHC Class II (M5114), CD19 (HB305) and CD4 (GK1.5), and goat anti-rat IgG-coated magnetic beads (QIAGEN, Victoria, Australia). Purity was 70–85% CD8^{+}Vα2^{+}Vβ5^{+} cells, determined by incubation with phycoerythrin (PE)-conjugated anti-Vα2 (B20.1), anti-Vβ5.1,5.2-biotin (MR9-4) and anti-CD8-fluorescein isothiocyanate (FITC) (53-6.7) mAb with streptavidin-PE-Cy5 (all from Becton Dickinson, NSW, Australia) and analysis using a FACSCalibur with CellQuest version 3.1f software (Becton Dickinson). Recipient B6.SJL/J-Ptprc^{a} mice received 1 – 2x10^{6} OT-I cells intravenously in 200 μL saline, 24 h before priming with sex-matched OVA-coated splenocytes.

OVA-coated splenocytes were prepared as described [35] with modifications [36] by incubating naïve adult B6.SJL/J-Ptprc^{a} spleen cells with 10 mg/mL OVA (Sigma, NSW, Australia) for 10 min at 37°C then irradiating at 3000 cGy. Mice were injected with 40x10^{6} OVA-coated splenocytes in 200 μL saline subcutaneously at the base of the tail.

Analysis and purification of naïve, effector and memory cells by flow cytometry

Naïve OT-I cells were purified from pooled inguinal, aortic and axillary LN of untreated OT-I mice based on the phenotype $CD8^+CD62L^{high}$ (MFI >200, >95% of population) and $CD44^{low}$ (lowest 15% of $CD45.2^+CD8^+CD62L^{high}$ population). Effector OT-I cells were purified from draining (inguinal and lumbar) LN of B6.SJL/J-$Ptprc^a$ mice following adoptive transfer and priming, based on the phenotype $CD45.2^+CD8^+CD44^{high}$ (MFI >200, >90%) and $CD62L^{low}$ (MFI <10, 10% of $CD45.2^+CD8^+CD44^{high}$ cells). Memory OT-I cells were purified from spleens of B6.SJL/J-$Ptprc^a$ mice following adoptive transfer and priming, by depleting MHC Class II^+, $CD19^+$ and $CD4^+$ cells then analyzing or sorting $CD45.2^+CD8^+CD44^{high}$ (MFI >200, >90%) cells. Where indicated, memory OT-I cells were further separated as follows: $CD62L^{high}$ (MFI >200, 60% of the population) and $CD62L^{low}$ (MFI <100, 10%); $CD122^{high}$ (MFI >150, 30%) and $CD122^{low}$ (MFI <50, 6%); $CD127^{high}$ (MFI >150, 10%) and $CD127^{low}$ (MFI <50, 10%); $Ly6C^{high}$ (MFI >100, 80%) and $Ly6C^{low}$ (MFI <10, 4%).

The following mAb were used: anti-CD45.2-FITC or -allophycocyanin (104), anti-CD8-PE-Cy5 (53-6.7), anti-CD44-biotin (IM.7), anti-CD62L-PE or -FITC (MEL-14) mAb and streptavidin-PE-Cy7 (Becton Dickinson), and anti-CD62L-FITC, anti-CD122-FITC, anti-CD127-FITC or anti-Ly6C-FITC (BioLegend, San Diego, USA). Lymphocytes were gated on forward/side scatter with dead cell exclusion using PI (Calbiochem, Victoria, Australia). Positive mAb staining was defined with reference to isotype control Ab staining. Cells were sorted using a MoFlo cytometer (DakoCytomation, Glostrup, Denmark) with Summit software V4.3 (DakoCytomation) or analyzed using a FACSCalibur with CellQuest version 3.1f software (Becton Dickinson).

Assays for cytolytic function

All cultures were performed in Dulbecco's modified Eagle's medium supplemented with 5% heat-inactivated FCS, 2 mM glutamine, $5x10^{-5}$ M 2-mercaptoethanol, 100 U/mL penicillin and 100 μg/mL streptomycin (complete DMEM). To measure degranulation, cells were restimulated in vitro with immobilized anti-CD3ε mAb (145-2C11, coated at 1 μg/mL for effector cells and 10 μg/mL for memory cells) in the presence of FITC-labeled mAb to CD107a and CD107b mAb (BioLegend) or isotype control Ab, and brefeldin A (10 μg/mL) (Sigma). After 4 h, cells were washed and analyzed by flow cytometry.

To assay cytolytic activity, draining LN cells from OVA-primed mice were re-stimulated in vitro with 10 μg/mL $OVA_{257-264}$ peptide SIINFEKL and 20 U/mL human recombinant interleukin-2 (rIL-2; NIH AIDS Research and Reference Reagent Program, Germantown, MD) in complete DMEM at 37C° in 5% CO_2 for 5 days then centrifuged on Ficoll-Hypaque. EL4 target cells were incubated with or without 20 μg/mL SIINFEKL peptide, labeled with 100 μCi $Na^{51}CrO_4$ (Amersham, NSW, Australia), washed and $2x10^3$ cells added to round-bottom 96-well plates (BD Falcon, NSW, Australia) with triplicate serial dilutions of effector cells in 200 μL complete DMEM [36]. After incubation for 4.5 h at 37°C in 5% CO_2, supernatants were assayed for γ-emission in 96-well Lumaplates (Perkin Elmer, Australia). Percent specific lysis was calculated as: 100 x [(mean sample cpm – mean spontaneous cpm)/(mean maximal cpm – mean spontaneous cpm)]. Maximal cpm corresponds to target cell lysis with 10% sodium dodecyl sulfate; spontaneous cpm corresponds to target cell lysis without effector cells.

Tumor protection experiments

Naïve OT-I cells ($1 – 2x10^6$) were adoptively transferred intravenously into B6.SJL/J-$Ptprc^a$ mice. One day later, recipient mice were primed by injection of $40x10^6$ OVA-coated splenocytes in 200 μL saline subcutaneously at the base of the tail. Three months later, control (unprimed) and primed

recipient mice were challenged with $5x10^6$ cells of the OVA-expressing EL-4 tumor EG.7 [36] subcutaneously at the base of the tail. Tumor size was monitored every three days and mice were culled when tumors reached 10 mm x 10 mm.

Clonal and paired daughter analyses of $CD8^+$ T cells

Terasaki microwells were coated with protein G-purified mAb to CD8α (53.6; 10 μg/mL), CD11a (I21/7.7; 5 μg/mL) and CD3ε (145-2C11; 2 μg/mL for effector cell cultures or 10 μg/mL for naïve and memory cell cultures, unless otherwise indicated) [12]. For cloning experiments, single purified naive, effector or memory OT-I cells were deposited using the single-cell deposition unit attached to a FACS Vantage (Becton Dickinson) into the Ab-coated wells containing complete DMEM and 20 U/mL human rIL-2 with or without 100 U/mL IL-4 (ProsPec-Tany TechnoGene, Rehovot, Israel). After 5 days, all wells were screened for clones and the cell number per clone was estimated microscopically. Cloning efficiency was defined as the percentage of single cells cultured that formed clones.

For paired daughter analysis, single naïve, effector or memory cells were deposited as above into anti-CD3/8/11a Ab-coated Terasaki wells containing complete DMEM with IL-2. After 2 days, wells were checked for viable cells and, where a parent cell had divided once, individual daughters were transferred by micromanipulation using a drawn-out capillary pipette into new Ab-coated Terasaki wells, one cell with IL-2 and one with IL-2 plus IL-4 as above [12]. Five days later, wells were screened for subclones and cell numbers per subclone were estimated.

RNA was obtained from clones and subclones by lysis with Nonidet P-40, reverse-transcribed and PCR-amplified in two rounds of 40 and 30 cycles with nested primers [12]. Products were agarose-electrophoresed and visualized by ethidium bromide DNA staining. Each PCR run included a

dilution series of cloned cDNAs for CD3ε, IFN-γ and IL-4 and a minimum of six negative control (water) samples. The sensitivity of each reaction was $\leq 10^{-16}$ g cDNA.

Re-activation of memory CD8$^+$ T cells in vivo and analysis by real-time PCR

Memory or naïve OT-I cells were co-injected with $40x10^6$ cells of the IL-4-secreting or control (empty vector) EG.7 tumor [36, 37] into RAG-$1^{-/-}$ mice subcutaneously at the base of the tail. After 5 days, $CD8^+$ $CD44^{high}CD62L^{low}$ OT-I cells were purified from pooled draining LN and spleens, and triplicate samples of 1000 cells were lysed with Nonidet P-40. Following mRNA extraction and cDNA synthesis, β2-microglobulin (β2M), IFN-γ and IL-4 cDNAs were quantified using real-time PCR as described [20]**.** Absolute cDNA copy numbers were determined by reference to standard curves generated with known copy numbers of cloned cDNAs and expressed as β2M units [(target gene copy number/β2M copy number) $x10^4$].

Statistical analysis

Data were analyzed by unpaired *t*-test or Fisher's exact test (Prism 4.02 software package, GraphPad Software 1) and differences were considered significant when $p<0.05$.

Acknowledgements: We thank Dr William Heath for the generous gift of mice, the QIMR flow cytometry facility for cell sorting and QIMR animal facility staff for animal husbandry. The following reagent was obtained through the AIDS Research and Reference Reagent Program, Division of AIDS, National Institute of Allergy and Infectious Diseases, National Institutes of Health: human rIL-2 from Dr Maurice Gately, Hoffmann-LaRoche (Nutley, NJ). This work was supported by grants from the National Health and Medical Research Council (A.B. and A.K.) and the Cooperative Research Centre for Vaccine Technology (A.K.). The Cooperative Research Centre for Vaccine Technology was established and supported under the Australian Government's Cooperative Research Centres Programme. S.H.A. was supported by an Australian Postgraduate Award and the Basil Shaw Fellowship of the Australian Rotary Health Research Fund. A.B., P.G. and K.B. performed the experiments; S.H.A. and N.K. provided essential reagents and technical advice; A.K. supervised the study; A.B. and A.K. wrote the manuscript.

Conflict of interest: The authors declare no commercial or financial conflict of interest.

References

[1] **Youngblood, B., Hale, J.S. and Ahmed, R.,** Memory CD8 T cell transcriptional plasticity. F1000Prime Rep. 2015. **7**: 38 doi: 10.12703/P7-38.

[2] **Murphy, E., Shibuya, K., Hosken, N., Openshaw, P., Maino, V., Davis, K., Murphy, K. and O'Garra, A.,** Reversibility of T helper 1 and 2 populations is lost after long-term stimulation. J. Exp. Med. 1996. **183**: 901-913.

[3] **Grogan, J. L., Mohrs, M., Harmon, B., Lacy, D. A., Sedat, J. W. and Locksley, R. M.,** Early transcription and silencing of cytokine genes underlie polarization of T helper cell subsets. Immunity 2001. **14**: 205-215.

[4] **Wilson, C. B., Rowell, E. and Sekimata, M.,** Epigenetic control of T-helper-cell differentiation. Nat. Rev. Immunol. 2009. **9**: 91-105.

[5] **Swain, S. L.,** Generation and in vivo persistence of polarized Th1 and Th2 memory cells. Immunity 1994. **1**: 543-552.

[6] **Krawczyk, C. M., Shen, H. and Pearce, E. J.,** Functional plasticity in memory T helper cell responses. J. Immunol. 2007. **178**: 4080-4088.

[7] **Lohning, M., Hegazy, A. N., Pinschewer, D. D., Busse, D., Lang, K. S., Hofer, T., Radbruch, A. et al.,** Long-lived virus-reactive memory T cells generated from purified cytokine-secreting T helper type 1 and type 2 effectors. J. Exp. Med. 2008. **205**: 53-61.

[8] **Wei, G., Wei, L., Zhu, J., Zang, C., Hu-Li, J., Yao, Z., Cui, K. et al.,** Global mapping of H3K4me3 and H3K27me3 reveals specificity and plasticity in lineage fate determination of differentiating $CD4^+$ T cells. Immunity 2009. **30**: 155-167.

[9] **Hegazy, A. N., Peine, M., Helmstetter, C., Panse, I., Frohlich, A., Bergthaler, A., Flatz, L. et al.,** Interferons direct Th2 cell reprogramming to generate a stable GATA-3^{+}T-bet^{+} cell subset with combined Th2 and Th1 cell functions. Immunity 2010. **32**: 116-128.

[10] **Erard, F., Wild, M. T., Garcia-Sanz, J. A. and Le Gros, G.,** Switch of CD8 T cells to noncytolytic CD8^{-}CD4^{-} cells that make TH2 cytokines and help B cells. Science 1993. **260**: 1802-1805.

[11] **Kienzle, N., Buttigieg, K., Groves, P., Kawula, T. and Kelso, A.,** A clonal culture system demonstrates that IL-4 induces a subpopulation of noncytolytic T cells with low CD8, perforin, and granzyme expression. J. Immunol. 2002. **168**: 1672-1681.

[12] **Kelso, A. and Groves, P.,** A single peripheral CD8^{+} T cell can give rise to progeny expressing type 1 and/or type 2 cytokine genes and can retain its multipotentiality through many cell divisions. Proc. Natl. Acad. Sci. U S A 1997. **94**: 8070-8075.

[13] **Lemaitre, F., Moreau, H. D., Vedele, L. and Bousso, P.,** Phenotypic CD8^{+} T cell diversification occurs before, during, and after the first T cell division. J. Immunol. 2013. **191**: 1578-1585.

[14] **Doyle, A. G., Buttigieg, K., Groves, P., Johnson, B. J. and Kelso, A.,** The activated type 1-polarized CD8^{+} T cell population isolated from an effector site contains cells with flexible cytokine profiles. J. Exp. Med. 1999. **190**: 1081-1092.

[15] **Yen, H. R., Harris, T. J., Wada, S., Grosso, J. F., Getnet, D., Goldberg, M. V., Liang, K. L. et al.,** Tc17 CD8 T cells: functional plasticity and subset diversity. J. Immunol. 2009. **183**: 7161-7168.

[16] **Jia, Y., Takeda, K., Han, J., Joetham, A., Marcus, R. A., Lucas, J. J., O'Connor, B. P. and Gelfand, E. W.,** Stepwise epigenetic and phenotypic alterations poise $CD8^+$ T cells to mediate airway hyperresponsiveness and inflammation. J. Immunol. 2013. **190**: 4056-4065.

[17] **Harland, K. L., Day, E. B., Apte, S. H., Russ, B. E., Doherty, P. C., Turner, S. J. and Kelso, A.,** Epigenetic plasticity of *Cd8a* locus during $CD8^+$ T-cell development and effector differentiation and reprogramming. Nat. Commun. 2014. **5**: 3547.

[18] **Cerwenka, A., Carter, L. L., Reome, J. B., Swain, S. L. and Dutton, R. W.,** In vivo persistence of CD8 polarized T cell subsets producing type 1 or type 2 cytokines. J. Immunol. 1998. **161**: 97-105.

[19] **MacDonald, H. R., Casanova, J. L., Maryanski, J. L. and Cerottini, J. C.,** Oligoclonal expansion of major histocompatibility complex class I-restricted cytolytic T lymphocytes during a primary immune response in vivo: direct monitoring by flow cytometry and polymerase chain reaction. J. Exp. Med. 1993. **177**: 1487-1492.

[20] **Olver, S., Groves, P., Buttigieg, K., Morris, E. S., Janas, M. L., Kelso, A. and Kienzle, N.,** Tumor-derived interleukin-4 reduces tumor clearance and deviates the cytokine and granzyme profile of tumor-induced $CD8^+$ T cells. Cancer Res. 2006. **66**: 571-580.

[21] **Sallusto, F., Geginat, J. and Lanzavecchia, A.,** Central memory and effector memory T cell subsets: function, generation, and maintenance. Annu. Rev. Immunol. 2004. **22**: 745-763.

[22] **Surh, C. D., Boyman, O., Purton, J. F. and Sprent, J.,** Homeostasis of memory T cells. Immunol. Rev. 2006. **211**: 154-163.

[23] **Hanninen, A., Maksimow, M., Alam, C., Morgan, D. J. and Jalkanen, S.,** Ly6C supports preferential homing of central memory $CD8^+$ T cells into lymph nodes. Eur. J. Immunol. 2011. **41**: 634-644.

[24] **Opferman, J. T., Ober, B. T. and Ashton-Rickardt, P. G.,** Linear differentiation of cytotoxic effectors into memory T lymphocytes. Science 1999. **283**: 1745-1748.

[25] **Kedzierska, K., Stambas, J., Jenkins, M. R., Keating, R., Turner, S. J. and Doherty, P. C.,** Location rather than CD62L phenotype is critical in the early establishment of influenza-specific $CD8^+$ T cell memory. Proc. Natl. Acad. Sci. U S A 2007. **104**: 9782-9787.

[26] **Chang, J. T., Palanivel, V. R., Kinjyo, I., Schambach, F., Intlekofer, A. M., Banerjee, A., Longworth, S. A. et al.,** Asymmetric T lymphocyte division in the initiation of adaptive immune responses. Science 2007. **315**: 1687-1691.

[27] **Gerlach, C., van Heijst, J. W., Swart, E., Sie, D., Armstrong, N., Kerkhoven, R. M., Zehn, D. et al.,** One naive T cell, multiple fates in $CD8^+$ T cell differentiation. J. Exp. Med. 2010. **207**: 1235-1246.

[28] **Russ, B. E., Olshanksy, M., Smallwood, H. S., Li, J., Denton, A. E., Prier, J. E., Stock, A. T. et al.,** Distinct epigenetic signatures delineate transcriptional programs during virus-specific $CD8^+$ T cell differentiation. Immunity 2014. **41**: 853-865.

[29] **Fitzpatrick, D. R., Shirley, K. M. and Kelso, A.,** Cutting edge: Stable epigenetic inheritance of regional IFN-γ promoter demethylation in $CD44^{high}CD8^+$ T lymphocytes. J. Immunol. 1999. **162**: 5053-5057.

[30] **Kersh, E. N., Fitzpatrick, D. R., Murali-Krishna, K., Shires, J., Speck, S. H., Boss, J. M. and Ahmed, R.,** Rapid demethylation of the *IFN-γ* gene occurs in memory but not naive CD8 T cells. J. Immunol. 2006. **176**: 4083-4093.

[31] **Denton, A. E., Russ, B. E., Doherty, P. C., Rao, S. and Turner, S. J.,** Differentiation-dependent functional and epigenetic landscapes for cytokine genes in virus-specific $CD8^+$ T cells. Proc. Natl. Acad. Sci. U S A 2011. **108**: 15306-15311.

[32] **Araki, Y., Wang, Z., Zang, C., Wood, W. H., Schones, D., Cui, K., Roh, T. Y. et al.,** Genome-wide analysis of histone methylation reveals chromatin state-based regulation of gene transcription and function of memory $CD8^+$ T cells. Immunity 2009. **30**: 912-925.

[33] **Cuddapah, S., Barski, A. and Zhao, K.,** Epigenomics of T cell activation, differentiation, and memory. Curr. Opin. Immunol. 2010. **22**: 341-347.

[34] **Hogquist, K. A., Jameson, S. C., Heath, W. R., Howard, J. L., Bevan, M. J. and Carbone, F. R.,** T cell receptor antagonist peptides induce positive selection. Cell 1994. **76**: 17-27.

[35] **Li, M., Davey, G. M., Sutherland, R. M., Kurts, C., Lew, A. M., Hirst, C., Carbone, F. R. and Heath, W. R.,** Cell-associated ovalbumin is cross-presented much more efficiently than soluble ovalbumin in vivo. J. Immunol. 2001. **166**: 6099-6103.

[36] **Baz, A., Buttigieg, K., Zeng, W., Rizkalla, M., Jackson, D.J., Groves, P. and Kelso, A.,** Branched and linear lipopeptide vaccines have different effects on primary $CD4^+$ and $CD8^+$ T-cell activation but induce similar tumor-protective memory $CD8^+$ T-cell responses. Vaccine 2008. **26**: 2570-2579.

[37] **Apte, S. H., Baz, A., Groves, P., Kelso, A. and Kienzle, N.,** Interferon-γ and interleukin-4 reciprocally regulate CD8 expression in $CD8^+$ T cells. Proc. Natl. Acad. Sci. U S A 2008. **105**: 17475-17480.

Figure Legends

Figure 1. Activation of effector $CD8^+$ T cells in vivo. B6.SJL/J-$Ptprc^a$ mice were adoptively transferred with 1 – $2x10^6$ naïve OT-I cells and primed one day later with $40x10^6$ irradiated OVA-coated B6.SJL/J-$Ptprc^a$ splenocytes. (A) At the indicated times after priming, $CD45.2^+CD8^+CD44^{high}$ $CD62L^{low}$ (activated OT-I) cell numbers and percentages among $CD45.2^+CD8^+$ (OT-I) cells were determined in draining LN by flow cytometry. Results are shown for one of two independent experiments as the arithmetic mean ± SD for 3 mice per time point. (B) At day 5 after priming, activated OT-I cells were purified from draining LN and assayed for degranulation by restimulation with anti-CD3 Ab in the presence of FITC-labeled anti-CD107a and anti-CD107b Ab (top panel) or isotype control Ab (lower panel) and brefeldin A, and analysis by flow cytometry. Representative histograms are shown for one of 3 samples. The percentage of positive cells defined by the indicated gate is shown. (C) At day 5 after priming, draining LN cells were restimulated in vitro with SIINFEKL peptide and IL-2 for 5 days then assayed for lytic activity in a ^{51}Cr-release assay with SIINFEKL-loaded or control EL-4 target cells. Results are shown from one of two experiments as mean ± SD for 5 mice where cells from each mouse were assayed separately in triplicate.

Figure 2. Phenotype and function of memory $CD8^+$ T cells. (A) Representative staining with mAb to CD44, CD62L, CD122, CD127 or Ly6C is shown for $CD8^+$ LN cells from untreated OT-I mice (left panels) and $CD45.2^+CD8^+$ spleen cells of B6.SJL/J-$Ptprc^a$ mice adoptively transferred with naïve OT-I cells, primed one day later with irradiated OVA-coated splenocytes and analyzed 60 days after priming (right panels). (B) Purified memory ($CD45.2^+CD8^+$ $CD44^{high}$) cells were assayed for degranulation by restimulation with anti-CD3 Ab in the presence of FITC-labeled anti-CD107a and anti-CD107b Ab (left panel) or isotype control Ab (right panel). Representative histograms are shown

for one of 3 samples. The percentage of positive cells defined by the indicated gate is shown. (C) OVA-coated splenocyte primed (n=10) or control unprimed (n=10) recipient B6.SJL/J-Ptprc^{a} mice were challenged with 5x10^{6} EG.7 cells 3 months after adoptive transfer of naïve OT-I cells. Mice were culled when tumors reached 10 mm x 10 mm size.

Figure 3. Paired daughter analysis to quantify IL-4 responsiveness of naïve, effector and memory CD8^{+} T cells. (A) Paired daughter analysis protocol. (B) CD3ε, IFN-γ and IL-4 mRNA expression by all tested subclones grown from daughters in IL-2 or IL-2+IL-4 as described in Table 2. Each row represents an expression pattern (filled, RNA positive; empty, RNA not detected). The number of subclones with each pattern is shown to the right of each row. Data are pooled from at least 3 independent experiments. (C) IL-4 mRNA expression by paired daughter subclones from B. Figures indicate the number of naïve, effector or memory parent cells which gave rise to a subclone pair with the indicated IL-4 expression pattern.

Figure 4. Functional plasticity of memory CD8^{+} T cells in vivo. Purified naïve OT-I LN cells (4x10^{4} in experiment 1, left; 5x10^{4} in experiment 2, right) or memory OT-I cells (5x10^{3}; 10^{4}) from spleens of B6.SJL/J-Ptprc^{a} mice 60 days after priming with irradiated OVA-coated splenocytes were adoptively transferred into RAG-1$^{-/-}$ recipients with 40 x 10^{6} control or IL-4-secreting EG.7 tumor cells. Five days later, effector cells were purified from pooled LN and spleens and analyzed for IL-4, IFN-γ and β2M mRNA by real-time PCR. Results of two independent experiments are shown, expressed as mean ± SD β2M units. Dotted line, threshold of IL-4 mRNA detection (0.3 units); ND, not detected.

Table 1. Clonal assessment of IL-4 responsiveness of naïve, effector and memory $CD8^+$ T cells[a]

Cell type	Naive		Effector		Memory	
Conditions	IL-2	IL-2+IL-4	IL-2	IL-2+IL-4	IL-2	IL-2+IL-4
No. cells cultured	576	576	576	576	576	576
Cloning efficiency	74 ± 15	74 ± 15	31 ± 5	36 ± 11	40 ± 4	60 ± 15
Clone size	236±86	256±90	154±87	232±81	175±87	179±92
No. clones analyzed	74	74	102	107	53	62
Size of analyzed clones	280±150	290±160	160±120	170±120	220±90	250±110
% $CD3\varepsilon^+$ clones	100	100	100	100	100	100
% IFN-γ^+ clones	100	100	100	100	100	100
% IL-4^+ clones	8 ± 6	96 ± 4	8 ± 4	19 ± 6	7 ± 5	84 ± 15

a) Purified naïve, effector (8 days after priming in vivo) and memory (3 months after priming in vivo) OT-I cells were cloned by culture of single cells with anti-CD3ε, -CD8 and -CD11a Ab in the presence of IL-2 or IL-2+IL-4. After 5 days, clone size was estimated and individual clones of a range of sizes were selected for analysis of CD3ε, IFN-γ and IL-4 mRNA expression by two-round nested PCR. Data are pooled from 3 independent experiments (mean ± SD).

Table 2. Paired daughter analysis of naïve, effector and memory $CD8^+$ T cells to measure IL-4 responsiveness[a]

	Naïve cells		Effector cells		Memory cells	
Primary culture conditions	IL-2		IL-2		IL-2	
No. parent cells cultured	1680		1800		2580	
% cultures with ≥2 cells on day 2	68 (40 – 85)		39 (30 – 55)		60 (53 – 75)	
Secondary culture conditions	IL-2	IL-2 + IL-4	IL-2	IL-2 + IL-4	IL-2	IL-2 + IL-4
No. cells transferred on day 2	207	207	219	219	386	386
% cells that subcloned by day 5	72	70	67	62	37	34
Mean subclone size on day 6 ± SD	501 ± 285	437 ± 285	93 ± 65	115 ± 75	96 ± 87	86 ± 88
No. subclones assayed by RT-PCR	102	102	131	131	95	95
% $CD3\varepsilon^+$ subclones	100	100	100	100	100	100

% IFN-γ^+ subclones	95	96	93	91	98	99
% IL-4^+ subclones	3	76	3	9	2	44
No. informative parent cells	102		131		95	
No. bipotential parent cells (frequency)	75 (73.5%)		8 (6.1%)		40 (42.1)	

a) Single naïve, effector and memory OT-I cells were cultured with anti-CD3/8/11a Ab and IL-2. After the first division, individual daughter cells were transferred into new Ab-coated wells, one with IL-2 and the other with IL-2+IL-4. Expression of CD3ε, IFN-γ and IL-4 mRNA was analyzed in all clone pairs by two-round nested PCR. Informative parent cells were those that gave rise to $CD3\varepsilon^+$ subclones in both IL-2 and IL-2+IL-4. Bipotential parent cells were those in which the subclone grown in IL-2 was $IL\text{-}4^-$ and the subclone grown in IL-2+IL-4 was $IL\text{-}4^+$. Data are pooled from at least 3 independent experiments.

Table 3. IL-4 responsiveness of memory $CD8^+$ T cell subpopulations[a]

Marker		High expression		Low expression	
		IL-2	IL-2 + IL-4	IL-2	IL-2 + IL-4
CD62L	No. cells cultured	420	420	360	360
	Cloning efficiency (day 5)	38 ± 7	47 ± 4	28 ± 8	32 ± 12
	Clone size ± SD	272 ± 322	360 ± 345	163 ± 208	190 ± 199
	No. clones analyzed	62	61	60	65
	% $CD3\varepsilon^+$ clones	100	100	100	100
	% IFN-γ^+ clones	97	100	77	77
	% IL-4^+ clones	0 (0 – 0)	61 (46 – 71)	7 (0 – 16)	47 (38 – 61)
CD122	No. cells cultured	240	240	240	240
	Cloning efficiency (day 5)	67 ± 17	70 ± 0	77 ± 7	73 ± 11
	Clone size ± SD	119 ± 66	151 ± 82	163 ± 81	158 ± 75
	No. clones analyzed	57	59	59	55
	% CD3 ε^+ clones	100	100	100	100
	% IFN- γ^+ clones	100	100	100	100

This is the author manuscript accepted for publication and has undergone full peer review but has not been through the copyediting, typesetting, pagination and proofreading process, which may lead to differences between this version and the Version of Record. Please cite this article as doi: 10.1002/eji.201545726.

% IL-4^{+} clones	9 (0 – 14)	83 (66 –100)	1 (0 – 3)	90 (73 – 87)

Continued overleaf

CD127	No. cells cultured	240	240	240	240
	Cloning efficiency (day 5)	60 ± 7	76 ± 9	71 ± 7	76 ± 10
	Clone size ± SD	136 ± 76	168 ± 90	160 ± 88	158 ± 112
	No. clones analyzed	62	62	65	65
	% CD3 ε^+ clones	100	100	100	100
	% IFN-γ^+ clones	100	98	100	100
	% IL-4^+ clones	1 (1 – 2)	79 (65 – 93)	7 (5 – 3)	89 (85 – 90)
Ly6C	No. cells cultured	300	300	300	300
	Cloning efficiency (day 5)	55 ± 12	66 ± 1	40 ± 20	42 ± 3
	Clone size ± SD	102 ± 81	128 ± 76	114 ± 75	144 ± 86
	No. clones analyzed	62	61	60	65
	% CD3ε^+ clones	100	100	100	100
	% IFN-γ^+ clones	ND	ND	ND	ND
	% IL-4^+ clones	4 (0 – 7)	62 (30 – 84)	19 (13 – 26)	71 (59 – 91)

a) Memory OT-I ($CD8^+CD45.2^+CD44^{high}$) cells from pooled spleens of 5 –10 adoptively-transferred mice 60 days after priming were purified based on high or low expression of the indicated marker, then cloned by single-cell culture with anti-CD3/8/11a Ab in the presence of IL-2 or IL-2+IL-4. After 5 days, expression of CD3ε, IFN-γ and IL-4 mRNAs was assayed in clones selected to match clone size between groups. Results are pooled from 3 independent experiments.

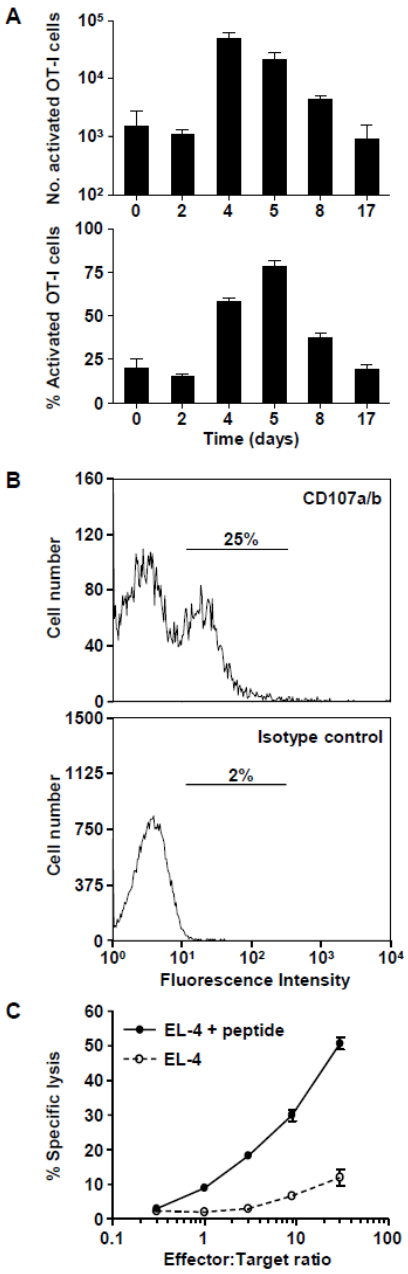

Baz et al. Figure 1

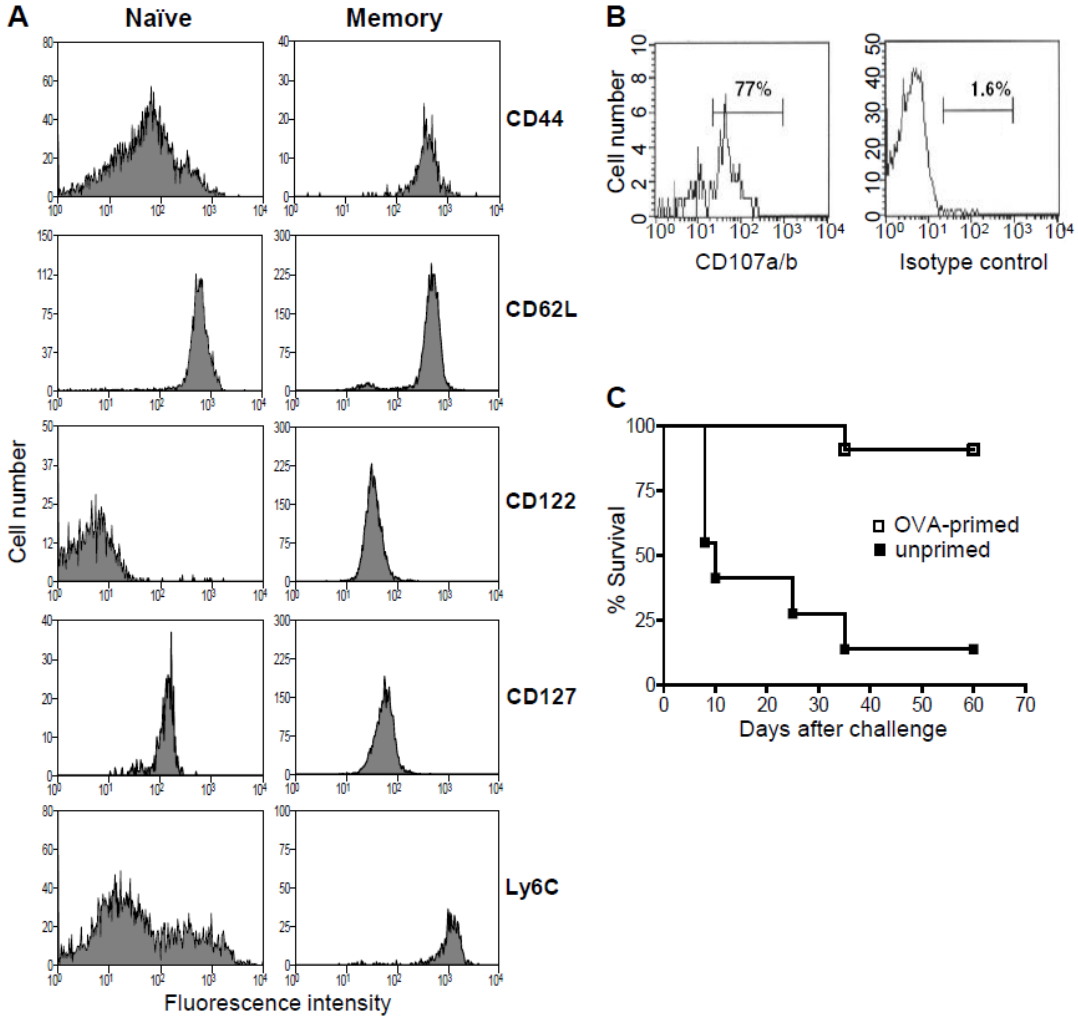

Baz et al. Figure 2

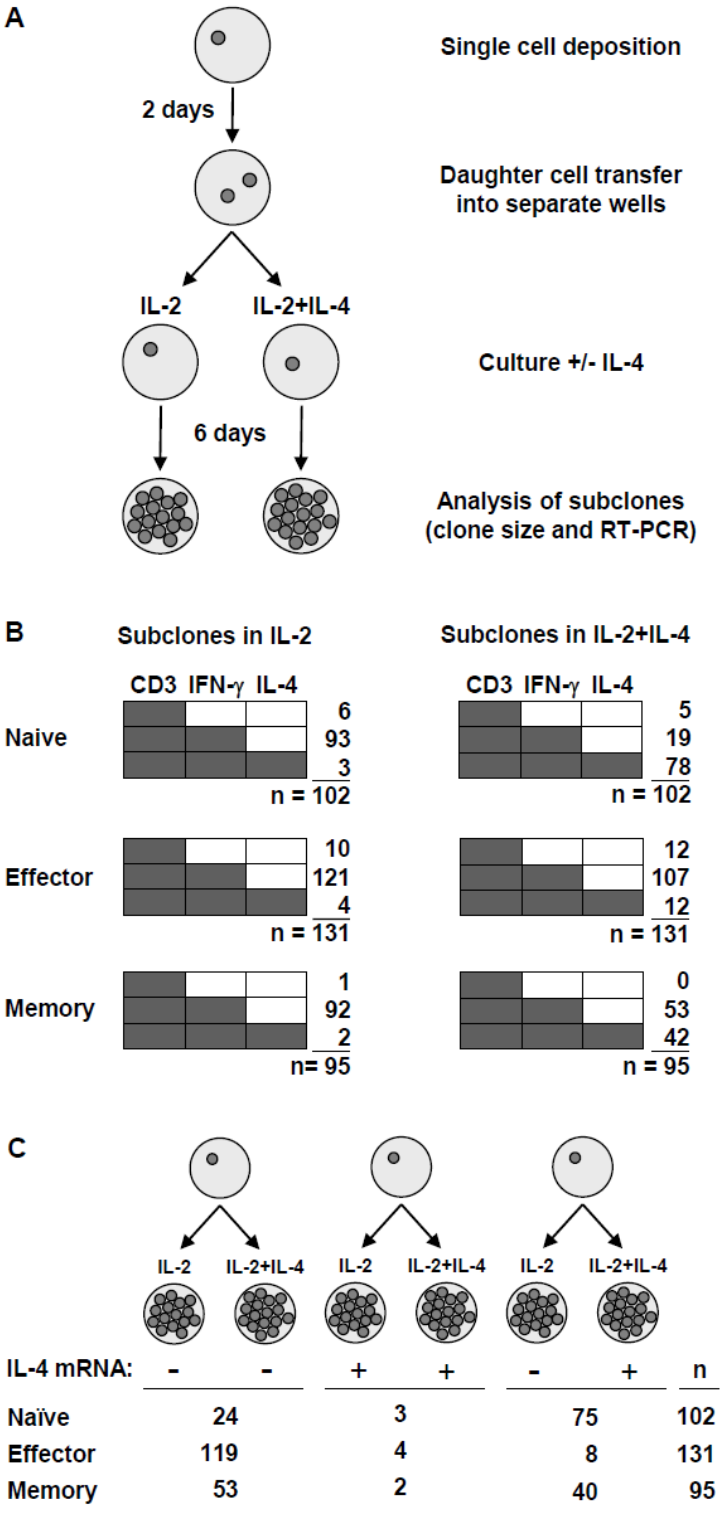

Baz et al. Figure 3

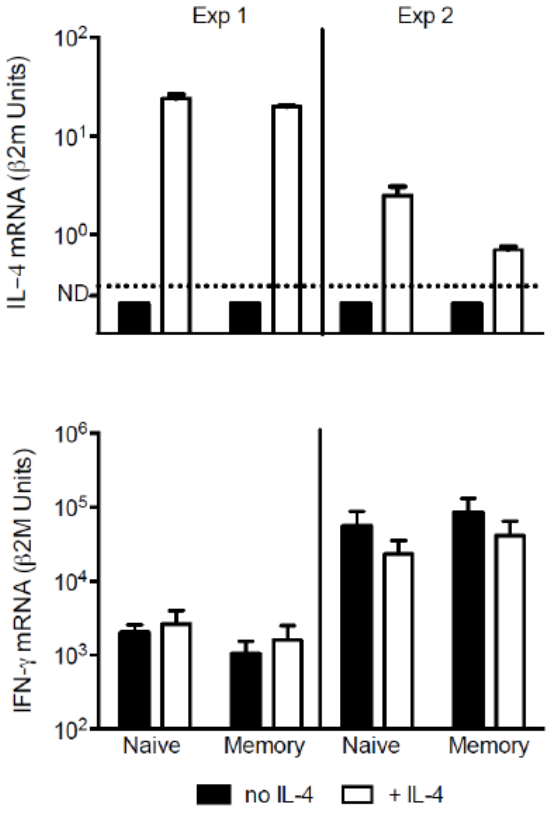

Baz et al. Figure 4

Author/s:
Baz, A; Groves, P; Buttigieg, K; Apte, SH; Kienzle, N; Kelso, A

Title:
Quantitative assessment of the functional plasticity of memory CD8(+) T cells

Date:
2016-04-01

Citation:
Baz, A., Groves, P., Buttigieg, K., Apte, S. H., Kienzle, N. & Kelso, A. (2016). Quantitative assessment of the functional plasticity of memory CD8(+) T cells. EUROPEAN JOURNAL OF IMMUNOLOGY, 46 (4), pp.863-873. https://doi.org/10.1002/eji.201545726.